Heat Mass Transfer (2009) 45:1383–1392
DOI 10.1007/s00231-009-0515-8

ORIGINAL

Transient heat conduction in two-dimensional functionally graded hollow cylinder with finite length

Masoud Asgari · Mehdi Akhlaghi

Received: 28 June 2008 / Accepted: 10 July 2009 / Published online: 26 July 2009

Abstract In this paper a thick hollow cylinder with finite length made of two dimensional functionally graded material (2D-FGM) subjected to transient thermal boundary conditions is considered. The volume fraction distribution of materials, geometry and thermal boundary conditions are assumed to be axisymmetric but not uniform along the axial direction. The finite element method with graded material properties within each element is used to model the structure and the Crank–Nicolson finite difference method is implemented to solve time dependent equations of the heat transfer problem. Two-dimensional heat conduction in the cylinder is considered and variation of temperature with time as well as temperature distribution through the cylinder are investigated. Effects of variation of material distribution in two radial and axial directions on the temperature distribution and time response are studied. The achieved results show that using two-dimensional FGM leads to a more flexible design so that transient temperature, maximum amplitude and uniformity of temperature distributions can be modified to achieve required specifications by selecting a suitable material distribution profile in two directions.

List of symbols

$c(r, z)$	Heat capacity of functionally graded material
c_0	Constant value
c_1, c_2	First ceramic and second ceramic
h_i, h_o, h_L, h_T	Convection coefficients at inner, outer, lower and upper surfaces
$k_r(r, z)$, $k_z(r, z)$	Thermal conductivity in the radial and axial directions
$[k_1]^e$, $[k_2]^e$, $[k_3]^e$	Characteristic matrices of elements
$[K_3]$, $[K]$	Global characteristic matrices
$[N(r, z)]$	Matrix of linear interpolation functions
n_r, n_z	Radial and axial power law exponents
m_1, m_2	First metal and second metal
$\{q\}^e$	Nodal temperature vector of element
$\{Q\}$	Global nodal temperature
r_i, r_o	Inner and outer radii
T_c	Constant value
T_∞	Surrounding temperature
V_{c_1}, V_{c_2}, V_{m_1}, V_{m_2}	Volume fractions of basic materials
$\rho(r, z)$	Mass density of functionally graded material

1 Introduction

In recent years, composition of several different materials is often used in structural components in order to optimize the thermal resistance and temperature distribution of structures subjected to thermal loading. For reducing the local stress concentration induced by abrupt transitions in material properties, the transition between different materials is made gradually. This idea used originally by Japanese researchers [1], leads to the concept of functionally graded materials (FGMs). These materials are expected to be used for thermal applications and high rate thermal loading. In the application of FGM cylindrical structures to aerospace, nuclear and automobile industries, analysis of transient heat transfer is of great importance. Analytical and computational studies of appointing thermal specifications

M. Asgari · M. Akhlaghi (✉)
Department of Mechanical Engineering, Amirkabir University of Technology, P.O. Box 15875-4413, Hafez Ave., Tehran, Iran
e-mail: makhlagi@aut.ac.ir

and temperature distribution in cylindrical structures made of FGM have been carried out by some researchers.

Temperature and stress distribution were determined in a stress-relief-type plate of FGMs with steady state and transient temperature distributions by Awaji [2]. A multi-layered material model was employed to solve the transient temperature field in a FGM strip with continuous and piecewise differentiable material properties by Jin [3]. A general analysis of one dimensional steady state heat conduction and thermal stresses in a thick hollow cylinder under axisymmetric and non-axisymmetric loads were developed by Jabbari et al. [4, 5]. A long boundary integral equation method with the moving least squares approximation was applied to transient heat conduction analysis in functionally graded material by Sladek et al. [6]. Tarn et al. [7] have studied the end effects of steady state heat conduction in a hollow or solid cylinder of FGM under two-dimensional thermal loads with arbitrary end conditions. The sensitivity analysis of heat conduction for functionally graded materials and the steady state and transient problem treated with the direct method and the adjoint method were presented by Chen et al. [8]. Transient temperature field and associated thermal stresses in FGM have been determined by using a finite element-finite difference method by Wang et al. [9]. A finite element-finite difference method was developed also to solve the time dependent temperature field in non-homogeneous materials such as FGMs by Wang and Tian [10]. Hosseini et al. [11] studied the one dimensional transient heat conduction in an infinite functionally graded cylinder using an analytical method. They derived the temperature distribution by using Bessel functions.

In all of the mentioned cases the variation of volume fraction and properties of the FGMs are one-dimensional and properties vary continuously from one surface to the other with a prescribed function while in advanced machine elements temperature and load distribution may change in two or three directions. Therefore, if the FGM has two-dimensional dependent material properties, more effective material resistance can be obtained. Based on this fact a two-dimensional FGM whose material properties are bi-directionally dependent is introduced [12]. Recently a few authors have investigated 2D-FGM. Cho and Ha [13] characterized thermoelastic behavior of heat resisting FGMs, under given thermal loading and boundary conditions by the spatial distribution of volume fractions of constituent particles. They addressed a two-dimensional volume-fraction optimization procedure for relaxing the effective thermal stress distribution. Modeling the backing shell of the cemented acetabular cup with 2D-FGM and comparing its performance in the reduction of stress against 1-D FGM cup was done by Hedia et al. [14]. Reduction of thermal stresses in a plate using 2D-FGMs was investigated by Alla [15]. In his study a 2D-FGM rectangular plate under transient thermal loading is considered and the finite element method has been used to solve the governing equations. Employing the finite element method is a common approach for solving problems of this nature in literatures. But it should be noted that conventional finite element formulations use a single material property for each element so the property field is constant within an individual element, leading to significant discontinuity and inaccuracies for transient and dynamic problems [16]. Refinement of element size can reduce this effect to some extent but not completely. These inaccuracies will be more significant in 2-D FGM cases. Sentare et al. [16] showed that graded finite element can improve accuracy without increasing the number of degrees of freedom and decreasing the size of elements. Based on these facts the graded finite elements method is preferred for modeling the 2D-FGM problems.

Analysis of transient heat conduction of a thick hollow functionally graded cylinder with finite length can be rarely seen in literatures. And also the heat conduction in finite length cylinder is often investigated only in radial direction in these cases, while in real situations the heat conduction can be two dimensional in a finite length cylinder. On the other hand in all cases the material gradation of FGM is one dimensional. Therefore analysis of transient heat conduction of a thick hollow cylinder made of 2-D FGM can be of great importance. In the present study, we consider a thick hollow cylinder with finite length made of 2D-FGM for which its material properties are varied in the radial and axial directions with a power law function. The thermal behavior of the structure under thermal boundary conditions introduced suddenly is considered. Variation of temperature with time, two-dimensional distribution of temperature through the cylinder in different times and the effect of material composition profile are analyzed. The volume fraction distribution, thermal load and cylinder geometry are assumed to be axisymmetric but not uniform along the axial directions. The effects of two-dimensional material distribution on the time response of the structure and temperature distribution are studied. The finite element method with graded material properties within each element is used to model the material properties variations. Material properties are calculated by using linear rule of mixtures and prescribed volume fraction in each point. The Crank–Nicolson finite difference method is used to solve governing equations of heat transfer problem in the time domain.

2 Problem formulation

In this section the governing equations of heat transfer in axisymmetric cylindrical coordinates are obtained. Volume

fraction distributions in the two radial and axial directions are introduced and graded finite element is used for modeling of the material non-homogeneity.

2.1 Governing equations

Consider a 2D-FGM thick hollow cylinder of internal radius r_i, external radius r_o, and finite length L. Because of axisymmetry of geometry and loading, coordinates r and z are used in the analysis.

2.1.1 Heat transfer equations

Without existence of heat sources, the equation of heat conduction in axisymmetric cylinder coordinates is obtained as

$$\frac{1}{r}\frac{\partial}{\partial r}\left(rk_r(r,z)\frac{\partial T(r,z,t)}{\partial r}\right)+\frac{1}{r}\frac{\partial}{\partial z}\left(rk_z(r,z)\frac{\partial T(r,z,t)}{\partial z}\right) = \rho(r,z)c(r,z)\frac{\partial T(r,z,t)}{\partial t} \quad (1)$$

where $k_r(r, z)$, $k_z(r, z)$, $\rho(r, z)$ and $c(r, z)$ are thermal conductivity in the radial and axial directions, mass density and heat capacity of functionally graded material, respectively, that vary in two directions. The thermal conductivities in the radial and axial directions are assumed to be the same.

The thermal boundary conditions are:

temperature at inner radius:

$$T(r_i,z,t)=T_c(1-e^{c_0 t})\sin\left(\frac{\pi z}{L}\right), \quad (2)$$

heat convection at the outer surface:

$$k_r\frac{\partial T(r_o,z)}{\partial r}+h_o(T-T_\infty)=0, \quad (3)$$

heat convection at the lower surface:

$$-k_z\frac{\partial T(r,0)}{\partial z}+h_L(T-T_\infty)=0 \quad (4)$$

heat convection at the top surface:

$$k_z\frac{\partial T(r,L)}{\partial z}+h_T(T-T_\infty)=0 \quad (5)$$

where h_o, h_L and h_T are convection coefficients in outer side, lower and upper surfaces, respectively. T_∞ is the surrounding temperature and T_c and c_0 are constant values. And the initial temperature of the cylinder is distributed uniformly.

2.2 Volume fraction and material distribution in 2D-FGM cylinder

Two-dimensional FGMs are usually made by continuous gradation of three or four distinct material phases in which one or two of them are ceramics and the others are metal alloy phases. The volume fractions of the constituents vary in a predetermined composition profile. Now consider the volume fractions of 2D-FGM at any arbitrary point in the 2D-FGM axisymmetric cylinder shown in Fig. 1. In the present cylinder the inner surface is made of two distinct ceramics and the outer surface from two metals.

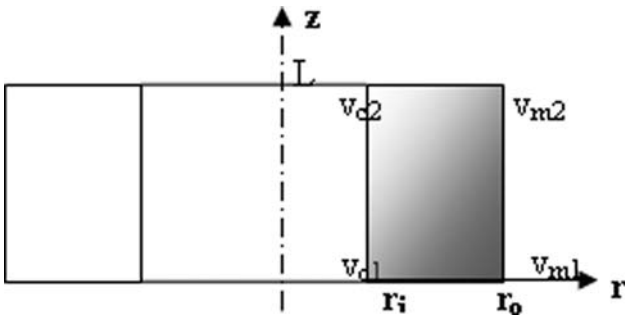

Fig. 1 Axisymmetric cylinder with two dimensional material distributions

The volume fraction of the first ceramic material is changed from 100% at the lower surface to zero at the upper surface by a power law function. Also this volume fraction is changed continuously from inner surface to the outer surface. Volume fractions of the other materials are changed similar to the one mentioned, in two directions. The volume fraction distributions of each material can be explained as:

$$V_{c_1}=\left[1-\left(\frac{r-r_i}{r_0-r_i}\right)^{n_r}\right]\left[1-\left(\frac{z}{L}\right)^{n_z}\right] \quad (6a)$$

$$V_{c_2}=\left[1-\left(\frac{r-r_i}{r_0-r_i}\right)^{n_r}\right]\left[\left(\frac{z}{L}\right)^{n_z}\right] \quad (6b)$$

$$V_{m_1}=\left(\frac{r-r_i}{r_0-r_i}\right)^{n_r}\left[1-\left(\frac{z}{L}\right)^{n_z}\right] \quad (6c)$$

$$V_{m_2}=\left(\frac{r-r_i}{r_0-r_i}\right)^{n_r}\left(\frac{z}{L}\right)^{n_z} \quad (6d)$$

where subscripts c_1, c_2, m_1, m_2 denote first ceramic, second ceramic, first metal and second metal respectively. Also n_r, n_z are non-zero parameters that represent the basic constituent distributions in r and z-directions. For instance, the volume fraction distribution of a basic material, c_1, for the typical values of $n_r = 2$ and $n_z = 3$ are shown in Fig. 2. In this case a thick hollow cylinder of inner radius $r_i = 1$ m, outer radius $r_o = 1.5$ m, and length $L = 1$ m is considered.

Material properties at each point can be obtained by using the linear rule of mixtures, in which a material property P at any arbitrary point (r, z) in the 2D-FGM cylinder is determined by linear combination of volume

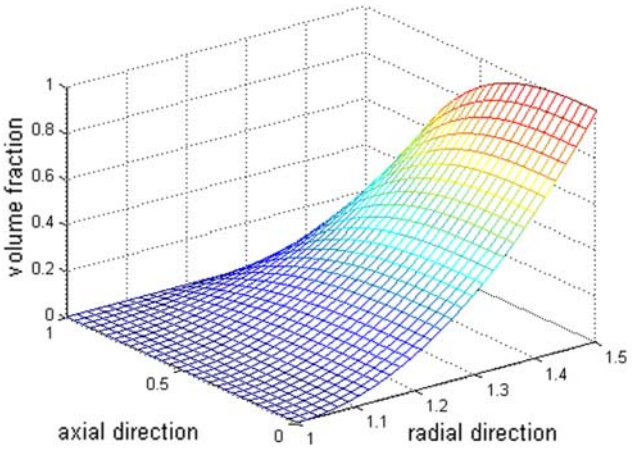

Fig. 2 Volume fraction distribution of m_1 for $n_r = 2$ and $n_z = 3$

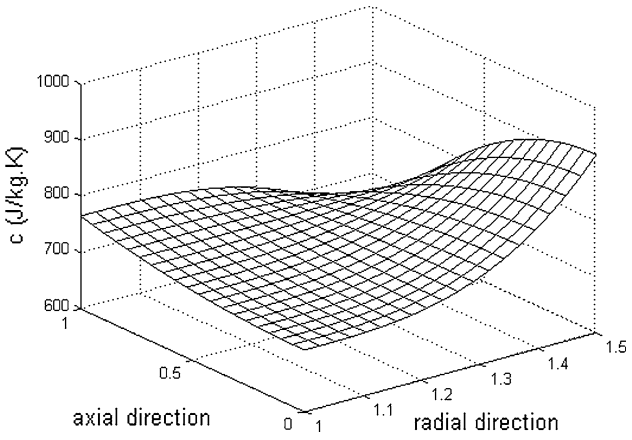

Fig. 3 Variation of specific heat capacity through the cylinder for $n_r = 2$ and $n_z = 3$

Table 1 Basic constituents of the 2D-FGM cylinder

Constituents	Material	ρ (kg/m^3)	K (W/mK)	c (J/kg K)
m_1	Al1100	2,715	220	917
m_2	Ti6Al4V	4,515	6	610
c_1	SiC	3,210	100	710
c_2	SiO_2	2,600	13	745

fractions and material properties of the basic materials as shown in the following equation:

$$P = P_{c_1} V_{c_1} + P_{c_2} V_{c_2} + P_{m_1} V_{m_1} + P_{m_2} V_{m_2} \tag{7}$$

The rule of mixtures is representative averaging estimate. This method is simple and convenient to apply for predicting the overall material properties and responses, however, owing to the assumed simplifications the validity is affected by the detailed microstructure and others. Because this estimate can not reflect the detailed constituent geometry, the dispersion structure and so on, its accuracy is well known to be highly questionable. But also it should be noted that most of the more precise methods are too complicated and many researchers considered them as the main problem for contribution [17, 18]. Also use of these models is usually developed for 1D-FGMs (two phase materials) and approximation models for 2D-FGMs are considered recently.

The basic constituents of the 2D-FGM cylinder are presented in Table 1:

The variation of a material property such as specific heat capacity based on the mentioned approach through the cylinder for the typical values of $n_r = 2$ and $n_z = 3$ is shown in Fig. 3.

2.3 Graded finite element modeling

In order to solve the governing equations the finite element modeling with graded element properties is used. To model a continuously non-homogeneous material, the material property function must be discretized according to the size of the element mesh. This approximation can provide significant discontinuities and these artificial discontinuities can cause enormous error in the results. Effects of these discontinuities will be more considerable in the 2D-FGMs because of its 2D non-homogeneity. Based on these facts the graded finite element is strongly preferable for modeling the present problem.

For modeling the heat transfer problem an axisymmetric ring element with triangular cross-section is used to discrete the domain. By taking the three nodal values of temperature as the degrees of freedom a linear model can be assumed as [19]:

$$T^e(r,z,t) = [N(r,z)]\{q\}^e, \tag{8}$$

where $[N]$ is the matrix of linear interpolation functions and$\{q\}^e$ is the nodal temperature vector of the element as

$$[N(r,z)] = [N_i(r,z)\ N_j(r,z)\ N_k(r,z)] \tag{9}$$

$$\{q\}^e = \{q_i\ q_j\ q_k\} \tag{10}$$

Additional information is provided in the Appendix.

The variational form of the present problem leads to the following minimized integral

$$I = 1/2 \iiint_V \left[k_r r \left(\frac{\partial T}{\partial r}\right)^2 + k_z r \left(\frac{\partial T}{\partial z}\right)^2 + 2\rho c T \frac{\partial T}{\partial t} \right] dv + 1/2 \iint_S h(T^2 - 2T_\infty T) ds \tag{11}$$

where V and S are the volume of the cylinder and the boundary on which the convective heat loss is specified.

The cylinder is now divided into the finite elements. The function I which is the sum of elemental quantities is minimized by using Eq. 8 subjected to the boundary and

initial conditions. The graded finite element equations for each element are then derived as

$$[k_1]^e\{q\}^e + [k_2]^e\{q\}^e + [k_3]^e\{\dot{q}\}^e = \{P_T\}^e \tag{12}$$

where

$$[k_1]^e = 2\pi \iiint_V r[B]^T[D(r,z)][B]dV \tag{13}$$

$$[k_2]^e = 2\pi \iint_S h \begin{Bmatrix} N_i \\ N_j \\ 0 \end{Bmatrix} [N_i \quad N_j \quad 0] rds \tag{14}$$

$$[k_3]^e = \iiint_V \rho(r,z)c(r,z)[N]^T[N]dV \tag{15}$$

$$\{P_T\}^e = \iint_S hT_\infty[N]^T ds \tag{16}$$

$$[B] = \begin{bmatrix} \frac{\partial N_i}{\partial r} & \frac{\partial N_j}{\partial r} & \frac{\partial N_h}{\partial r} \\ \frac{\partial N_i}{\partial z} & \frac{\partial N_j}{\partial z} & \frac{\partial N_h}{\partial z} \end{bmatrix} \tag{17}$$

$$[D(r,z)] = \begin{bmatrix} rk_r(r,z) & 0 \\ 0 & rk_z(r,z) \end{bmatrix} \tag{18}$$

For finding the characteristic matrices the integral must be taken over the elemental volume, considering the distribution function of material properties through each element.

Now by assembling the element matrices, the global matrix equation for the structure can be obtained as

$$[K_3]\left\{\dot{Q}\right\} + [K]\{Q\} = \{P_T\} \tag{19}$$

where $\{Q\}$ is the vector of nodal temperature of the cylinder and also

$$[K_3] = \sum_{e=1}^{M} [K_3]^e \tag{20}$$

$$[K] = \sum_{e=1}^{M} [K_1]^e + [K_2]^e \tag{21}$$

$$\{P_T\} = \sum_{e=1}^{M} \{P_T\}^e \tag{22}$$

where M is the number of elements. Once the finite elements equations are established, the Crank–Nicolson finite difference method [20] with a suitable time step is used to solve the equations.

3 Implementation and validation

To verify the present work, since similar works are few, we simplify the present problem to be similar to the published literatures. At first a finite length 1D functionally graded cylinder under steady thermal loading solved semi-analytically in Ref. [21] using the series solution is considered. Then an infinite 1D-FGM cylinder under transient thermal loading solved analytically using Bessel functions in Ref. [11] is employed for verification and comparison of the results.

3.1 Finite length 1D-FGM cylinder under steady thermal loading

Consider a thick hollow cylinder in which the material distribution in the radial direction varies from ceramic (Mullite) at the inner surface to metal (Molybdenum) at the outer surface with a power law function. The geometrical parameters are as follows: length $L = 5$ m, inner radius $r_i = 0.7$ m and outer radius $r_o = 1$ m. The temperature distributions along surfaces are [21]:

$$T(r_i,z) = T_o \sin\left(\frac{\pi z}{L}\right) \quad \text{at } r = r_i, \tag{23a}$$

$$T(r_o,z) = 0 \quad \text{at } r = r_o, \tag{23b}$$

$$T(r,0) = 0 \quad \text{at } z = 0, \tag{23c}$$

$$T(r,L) = 0 \quad \text{at } z = L, \tag{23d}$$

where $T_o = 200$°C and all temperatures are in °C. The governing equations can be solved using a multi-layer approach [21]. For solving the mentioned problem by the graded finite element method developed here as a transient problem, we suppose that the thermal boundary conditions exerts as initial condition and the material properties vary in radial direction only. Therefore responses after a long time can be considered as the steady state result. Convergence of the time response is analyzed and the time step is chosen such that the response doesn't depend on it. Also we suppose that the material properties vary in radial direction only and the volume fraction exponent and property coefficients are taken as: $n_z = 0$, $n_r = 5$, $P_{c_1} = P_{c_2} = P_c$ and $P_{m_1} = P_{m_2} = P_m$. where P_c is the material property of the inner surface which is considered to be ceramic and P_m is the material property of the metallic outer surface.

The variation of temperature with time in a specific point obtained using the present method and steady temperature of the same point obtained from the series solution [21] are shown in Fig. 4. The difference between the transient and the steady temperature is less than 10^{-5} after 6×10^4 s. So, comparison of the results shows good agreement between the two methods.

3.2 Infinite 1D-FGM cylinder under transient thermal condition

In this case the distribution of mechanical properties are considered one-dimensional and across the thickness of the

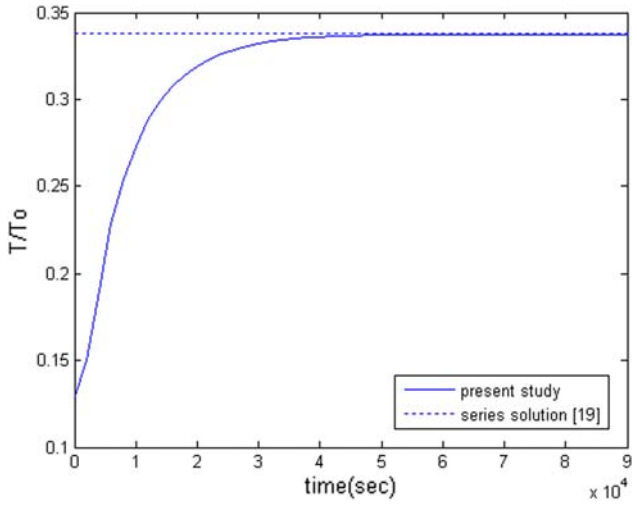

Fig. 4 Variation of temperature with time at $z/L = 0.5$, $r/r_o = 0.85$

FG cylinder. The initial condition and boundary conditions on inner and outer radii are assumed to be the same as [11]:

$$k_r \frac{\partial T(r_i, z, t)}{\partial r} + h_i(T - T_\infty) = 0 \quad \text{at } r = r_i, \tag{24a}$$

$$\frac{\partial T(r_o, z, t)}{\partial r} = 0 \quad \text{at } r = r_o, \tag{24b}$$

$$T(r, z, 0) = 200\,^\circ\text{C}, \tag{24c}$$

Material properties are the same and $r_o/r_i = 1.5$. In order to have radial heat conduction, thermal conductivity in the axial direction is eliminated. The cylinder is assumed to be too long and the temperature distribution along the radial direction is considered. The obtained results are then compared with the published data. The maximum difference for n.t = 0.5 and n.t = 2 are 0.82 and 0.74%, respectively. Figure 5 shows good agreement between the results at all points.

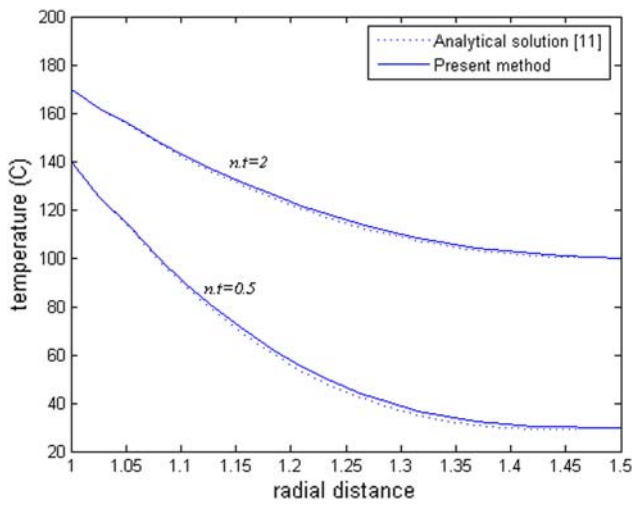

Fig. 5 Time history of temperature's radial distribution, *n.t* is the non-dimensional time

4 Numerical results and discussion

A thick hollow cylinder of inner radius $r_i = 1$ m, outer radius $r_o = 1.5$ m, and length $L = 1$ m made of FGM with two–dimensional gradation of distribution profile is investigated. Constituent materials are two distinct ceramics and two distinct metals described in Table 1. Volume fraction of materials is distributed according to Eq. 6. Responses for some different powers of material composition profiles n_r, n_z will be compared.

Thermal boundary conditions are:

$$T_i(z, t) = 1,000(1 - e^{c_0 t}) \sin(\pi z), \quad \text{at } r = r_i \tag{25}$$

$$k_r \frac{\partial T(r_o, z)}{\partial r} + h_o(T - T_\infty) = 0, \quad \text{at } r = r_o \tag{26}$$

$$-k_z \frac{\partial T(r, 0)}{\partial z} + h_L(T - T_\infty) = 0, \quad \text{at } z = 0 \tag{27}$$

$$k_z \frac{\partial T(r, L)}{\partial z} + h_T(T - T_\infty) = 0, \quad \text{at } z = 1 \tag{28}$$

$$T(r, z) = 25^\circ\text{C}, \quad \text{at } t = 0 \tag{29}$$

where, $h_o = h_L = h_T = 100$(J/kg K), $T_\infty = 25^\circ$C, $c_0 = -2$ and temperature unit is Centigrade.

In the following figures a cylinder with variation of volume fraction and material properties in two directions is considered. Figure 6 shows the temperature distribution through the cylinder at a specified time. The power law exponents of the material distribution profile in radial and axial directions are the same $n_r = n_z = 2$.

In order to have a more clear observation of effects of material distribution profile on transient responses, variation of temperature with time in two specified points near the upper and lower edges and two different points near the inner and outer surfaces of the cylinder are illustrated in Figs. 7 and 8 for different material distributions. In Fig. 7 the power law exponent in the radial direction is constant,

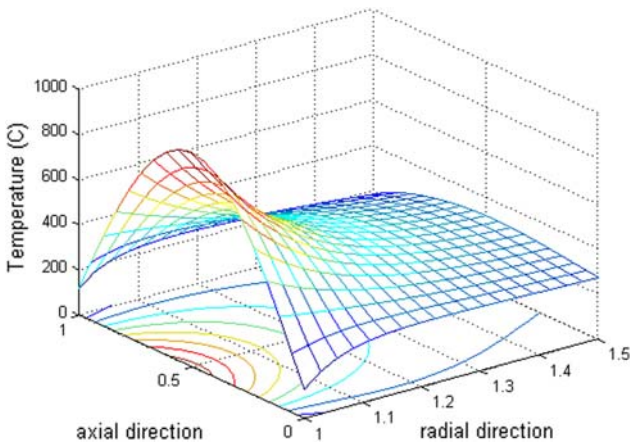

Fig. 6 Temperature distribution through the cylinder after 2,000 s

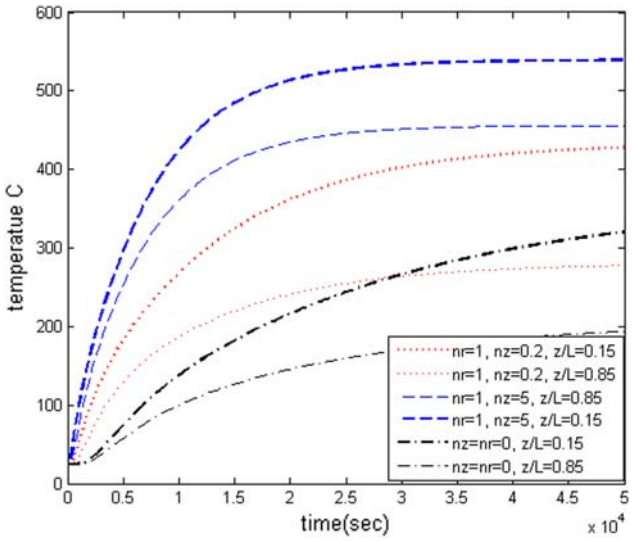

Fig. 7 Transient temperature at points near the up and down edges for different material distributions

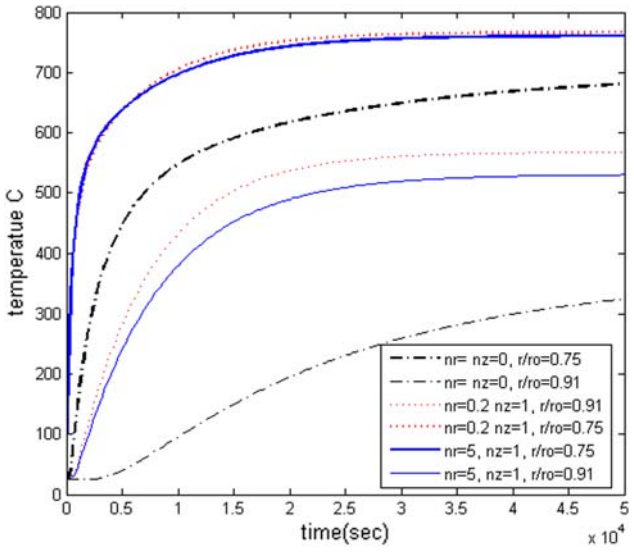

Fig. 8 Transient temperature at points near the inner and outer surfaces for different material distributions

but varies in the axial direction. Also the time response for a homogeneous cylinder ($n_r = n_z = 0$) is presented in this figure. In all of these cases the radial position of points are at $\left(\frac{r}{r_o} = 0.85\right)$. It is clear that the time responses are strongly affected by material distribution tailoring. Increasing the radial power law exponent, the steady temperature of the specified point increases and also the temperature will become steady sooner. As an example increasing n_z from 0.2 up to 5 in Fig. 7, increases the steady temperature by more than 25% at that specified point.

The same results are plotted for two different points near the inner and outer surfaces in Fig. 8. In these cases points

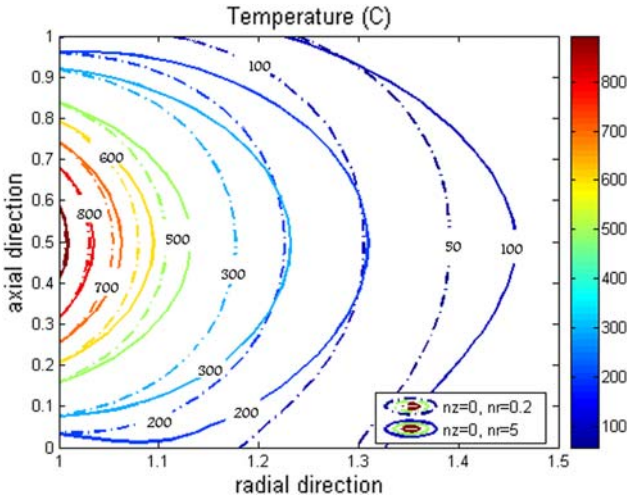

Fig. 9 Temperature distribution (C) through the radial FG cylinder after 100 s

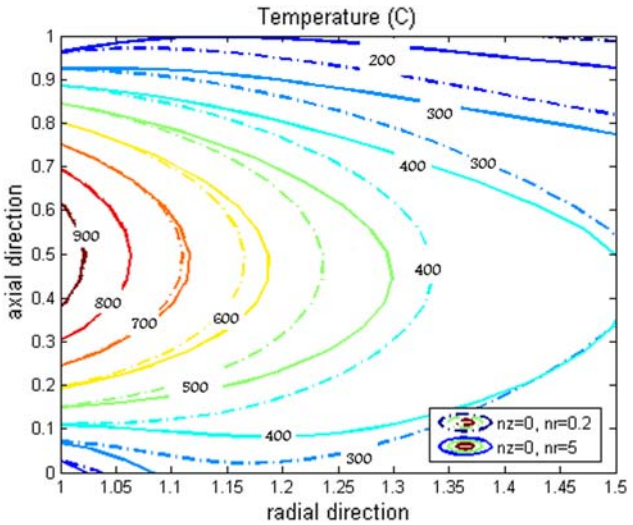

Fig. 10 Temperature distribution (C) through radial FG cylinder after 900 s

are located on $\frac{z}{L} = 05$.. Variation of temperature at the point located near the inner surface is less than the point near the outer surface of boundary condition at inner surface.

In order to have a more clear and comprehensive observation, distributions of temperature through the cylinder at different times are illustrated in Figs. 9, 10, 11 and 12 for various material compositions. The thermal initial and boundary conditions are as Eqs. 25–29 in these plots.

In Figs. 9 and 10 material distributions are graded only in radial direction. It can be seen that in the same conditions the temperature distribution is different. The lower the value of n_r, the lower the temperature is near the outer surface.

Volume fractions are graded in the two radial and axial directions in Figs. 11 and 12. Significantly different

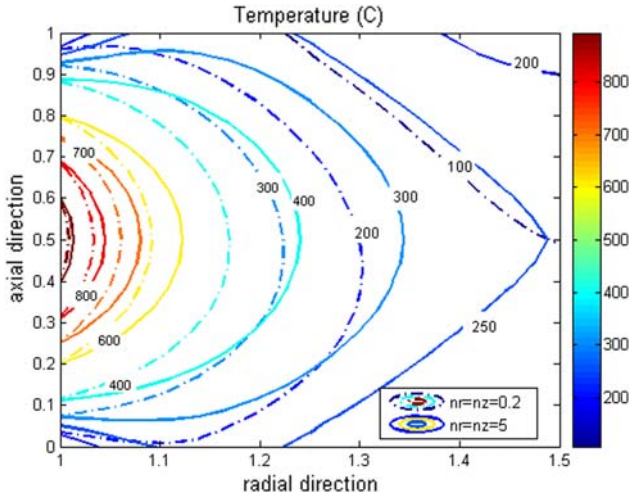

Fig. 11 Temperature distribution (C) through thme 2D-FGM cylinder for different material distributions after 100 s

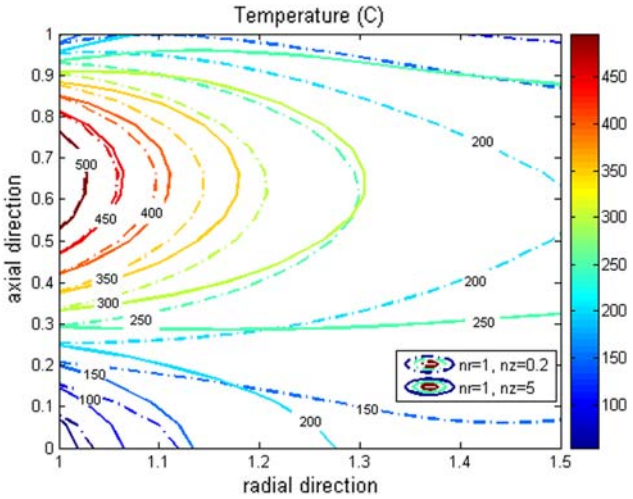

Fig. 13 Temperature distribution (C) through the 2D-FGM cylinder for different material distributions after 500 s

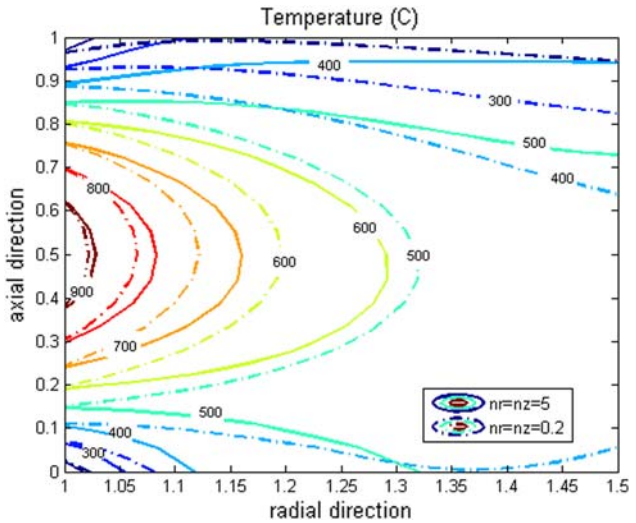

Fig. 12 Temperature distribution (C) through the 2D-FGM cylinder for different material distributions after 900 s

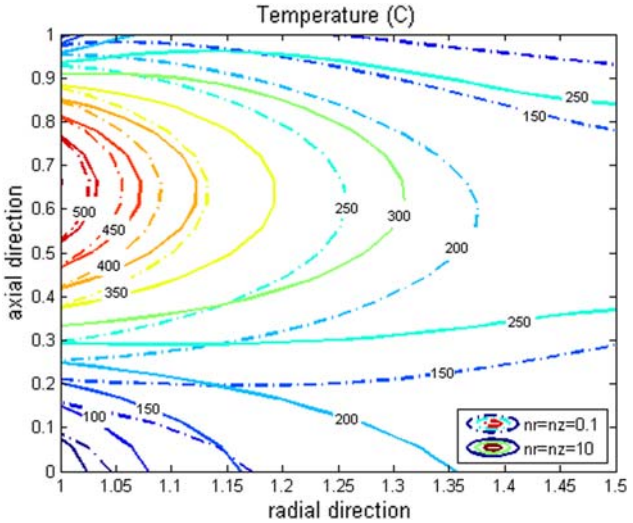

Fig. 14 Temperature distribution (C) through the 2D-FGM cylinder for different material distributions after 500 s

temperature distribution is obvious for the two specified times. For instance the temperature near the upper surface after 900 s is approximately 200°C for $n_r = n_z = 0.2$ while its value is more than 350°C for $n_r = n_z = 5$. Such different temperature distribution can be seen at the outer surface too.

Also the temperature distribution through the 2D-FGM cylinder in which the inner and upper surfaces are subjected to the following boundary conditions is considered.

$$T_i(z,t) = 100(1 - e^{c_0 t})z\sin(\pi z), \quad \text{at } r = r_i \tag{30}$$

$$k_z\frac{\partial T(r,L)}{\partial z} + h_T(T - T_\infty) = 0, \quad \text{at } z = 1 \tag{31}$$

where $T_\infty = 100$°C. As the thermal boundary conditions aren't symmetric with respect to the middle line in the axial direction in this case, two dimensional variations of materials distribution can be more effective to achieve a required temperature distribution. Figure 13 depicts the temperature distribution for two different values of n_r while the values of n_z are the same. Despite different temperature distributions a more effective change is expected. To this end the temperature distributions for two cases in which the volume fraction power exponents in radial and axial directions are different are illustrated in Fig. 14. Also two different values of power exponents are used in this case. So the temperature distribution is significantly affected and lower temperatures are achieved near the boundaries.

Radial distribution of temperature in the middle of the cylinder's length at a specified time ($t = 1{,}000$ s) is shown in the Fig. 15 for different material distributions. That

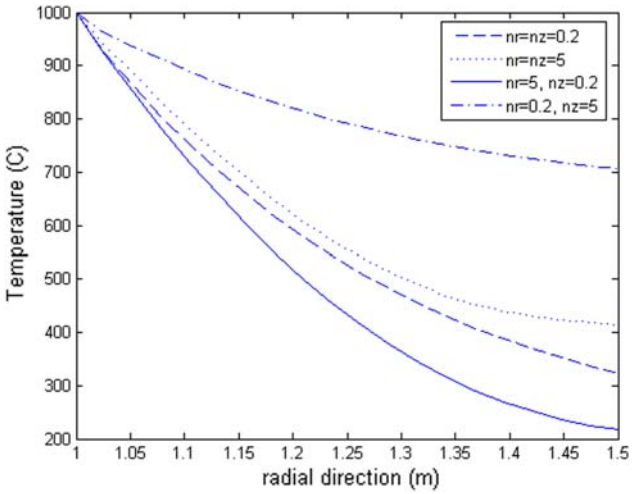

Fig. 15 Radial distribution of temperature for different material distributions on $z = 2.5$ after 1,000 s

clearly shows the difference between temperature distributions especially the temperature at the outer surface.

It is evident from these figures that both the magnitude and time delay of the responses are strongly affected by the material distribution powers n_r and n_z.

As it is seen in the results, temperature distribution and transient responses in two directions are strongly influenced by the material composition profile. In other words the time response, the maximum amplitude and the uniformity of temperature distribution through the cylinder can be modified to a required manner by selecting an appropriate material distribution profile. Variation of material distribution in two directions leads to a more flexible and desirable design which is very useful in optimization problems.

Although the manufacturing of multidimensional FGMs may seem to be costly or difficult, but it should be noted that while these technologies are relatively new, processes such as three-dimensional printing (3DP^{TM}) and Laser Engineering Net Shaping (LENS$^{(R)}$) can currently produce FGMs with relatively arbitrary tree-dimensional grading [22]. With further refinements FGM manufacturing methods may provide the designers with more control over the composition profile of functionally graded components with reasonable cost.

5 Conclusion

A two-dimensional functionally graded cylinder with finite length under transient thermal loading is studied. Heat conduction equations are considered in two radial and axial directions. For modeling and simulation of governing equations a graded finite element method was used that has some advantages to the conventional finite element method. The transient responses of 2D-FGM cylinder are developed and variations of different parameters with volume fraction exponents are obtained. Effects of two-dimensional material distribution on the temperature distribution and time responses are considered. Based on the achieved results, 2D-FGMs have a powerful potential for designing and optimization of structures under multi-functional requirements.

Appendix

The matrix of linear interpolation functions is

$$[N(r,z)] = [N_i(r,z) \quad N_j(r,z) \quad N_k(r,z)] \tag{32}$$

where subscripts i, j, k are related to three nodes of each element. And its components are

$$N_i = \frac{a_i + b_i r + c_i z}{2A}, \quad N_j = \frac{a_j + b_j r + c_j z}{2A}, \quad N_k = \frac{a_k + b_k r + c_k z}{2A} \tag{33}$$

where the constants a, b *and* c are defined in terms of the nodal coordinates as:

$$\begin{aligned} a_i &= r_j z_k - r_k z_j \\ a_j &= r_i z_k - r_k z_i \\ a_k &= r_i z_j - r_j z_i \\ b_i &= z_j - z_k \\ b_j &= z_k - z_i \\ b_k &= z_i - z_j \\ c_i &= r_j - r_k \\ c_j &= r_k - r_i \\ c_k &= r_i - r_j \end{aligned} \tag{34}$$

And A is the area of the element given by

$$A = 1/2(r_i z_j + r_j z_k + r_i z_k - r_k z_j) \tag{35}$$

Vector of nodal temperature (degrees of freedom) is

$$\{q\}^e = \begin{Bmatrix} T_i \\ T_j \\ T_k \end{Bmatrix} \tag{36}$$

References

1. Koizumi M (1993) The concept of FGM. Ceram Trans Funct Graded Mater 34:3–10
2. Awaji H (2001) Temperature and stress distributions in a plate of functionally graded materials. Fourth international congress on thermal stresses, June 8–11, Osaka, Japan
3. Jin ZH (2002) An asymptotic solution of temperature field in a strip of a functionally graded material. Int Common Heat Mass Transf 29:887–895

4. Jabbari M, Sohrabpour S, Eslami MR (2002) Mechanical and thermal stresses in a functionally graded hollow cylinder due to radially symmetric loads. Int J Press Vessel Pip 79:493–497
5. Jabbari M, Sohrabpour S, Eslami MR (2003) General solution for mechanical and thermal stresses in a functionally graded hollow cylinder due to nonaxisymmetric steady-state loads. ASME J Appl Mech 70:111–118
6. Sladek J, Sladek V, Zhang CH (2003) Transient heat conduction analysis in functionally graded materials by the meshless local boundary integral equation method. Comput Mater Sci 28:494–504
7. Tarn JQ, Wang YM (2004) End effects of heat conduction in circular cylinders of functionally graded materials and laminated composites. Int J Heat Mass Transf 47:5741–5747
8. Chen B, Tong L (2004) Sensitivity analysis of heat conduction for functionally graded materials. Mater Des 25:663–672
9. Wang BL, Mai YW, Zhang XH (2004) Thermal shock resistance of functionally graded materials. Acta Mater 52:4961–4972
10. Wang BL, Tian ZH (2005) Application of finite element–finite difference method to the determination of transient temperature field in functionally graded materials. Finite Elements Anal Des 41:335–349
11. Hosseini M, Akhlaghi M, Shakeri M (2007) Transient heat conduction in functionally graded thick hollow cylinders by analytical method. Heat Mass Transf. doi: 10.1007/s00231-006-0158
12. Abudi J, Pindera MJ (1996) Thermoelastic theory for the response of materials functionally graded in two directions. Int J Solid Struct 33:931–966
13. Cho JR, Ha DY (2002) Optimal tailoring of 2D volume-fraction distributions for heat-resisting functionally graded materials using FDM. Comput Method Appl Mech Eng 191:3195–3211
14. Hedia HS, Midany T, Shabara MAN, Fouda N (2005) Development of cementless metal-backed acetabular cup prosthesis using functionally graded material. Int J Mech Mater Des 2:259–267
15. Nemat-Alla M (2003) Reduction of thermal stresses by developing two dimensional functionally graded materials. Int J Solids Struct 40:7339–7356
16. Santare MH, Lambros J (2000) Use of a graded finite element to model the behavior of non-homogeneous materials. J Appl Mech 67:819–822
17. Gasik MM (1998) Micromechanical modelling of functionally graded materials. Comput Mater Sci 13:42–55
18. Cho JR, Ha DY (2001) Averaging and finite-element discretization approaches in the numerical analysis of functionally graded materials. Mat Sci Eng A302:187–196
19. Zienkiewicz OC, Taylor RL (2000) The finite element method, 5th edn. VII: Solid mechanics
20. Stasa FL (1985) Applied finite element analysis for engineers. CBS Publishing, Tokyo
21. Shao ZS (2005) Mechanical and thermal stresses of a functionally graded circular hollow cylinder with finite length. Int J Press Vessel Pip 82:155–163
22. Goupee AJ, Vel SS (2006) Two-dimensional optimization of material composition of functionally graded materials using meshless analyses and a genetic algorithm. Comput Methods Appl Mech Eng 195:5926–5948